Desalination and Water Treatment
www.deswater.com

doi: 10.5004/dwt.2017.21310

85 (2017) 330–338
August

Mesoporous treated sewage sludge as outstanding low-cost adsorbent for cadmium removal

H. Ait Ahsaine[a,*], M. Zbair[b], R. El Haouti[a]

[a]*Laboratoire Matériaux et Environnement LME, Faculté des Sciences, Université Ibn Zohr, BP 8106, Cité Dakhla, Agadir, Morocco, emails: a.hassan@uiz.ac.ma (H. Ait Ahsaine), r.elhaouti@gmail.com (R. El Haouti)*
[b]*Laboratoire de catalyse et corrosion des matériaux, Université Chouaib Doukkali, Faculté des sciences El Jadida, BP 20, El Jadida 24000, Morocco, email: zbair.mohamed@gmail.com*

Received 22 April 2017; Accepted 4 August 2017

ABSTRACT

Low-cost adsorbent based on sewage sludge was studied on the adsorption of cadmium ion (Cd(II)) in a batch system. The raw sewage sludge was treated using sulfuric acid and then heated at 300°C. The as-obtained material was characterized by thermogravimetric analyses, Fourier transform infrared spectroscopy, scanning electron microscopy and Brunauer–Emmett–Teller surface area. The treated sewage sludge (TSS) exhibits a higher surface area than the raw material due to the activation process. Some parameters such as adsorbent dose, solution pH, initial concentration and contact time were investigated in the batch system to study the optimum adsorption condition of the adsorbent. The kinetic study showed that the adsorption is well described by the pseudo-second-order kinetic model, while sorption isotherms gave better fit for the Langmuir model yielding an adsorption capacity of 56.2 mg/g. Moreover, adsorption mechanism was proposed on the basis of infrared spectroscopy and elemental analyses after adsorption.

Keywords: Adsorption; Heavy metals; Cadmium ions; Mesoporous; Sewage sludge

1. Introduction

Pollution with heavy metals has attracted public concern because it is one category of the most significant contaminants causing many environmental issues that threaten human health and ecological systems [1]. Large amounts of agricultural and industrial heavy metals are discharged everyday causing considerable contamination of ground water [2]. Cadmium ions have been recognized as a potential metallic toxicant by different international agencies including EEC black list and United Kingdom red list substances [3,4] and it becomes a serious threat because of its biological accumulation and solubility [5]. According to the US Environmental Protection Agency, the limit concentration of cadmium in drinking water is 0.005 mg/L [6], whereas the World Health Organization and American Water Works Association have recommended a limit of 0.003 mg/L [7].

Several methods have been used to sequester cadmium ions and heavy metals from aqueous solutions including membrane technology, ion exchange, phytoremediation, coagulation, chemical precipitation and ion exchange [8–11]. However, these methods have high operational costs, incomplete metal removal and enormous amount of residual sludge; so to overcome these drawbacks adsorption is considered a better choice, an inexpensive and eco-friendly method and it requires minimum skills for implementation.

Sewage sludge (SS) is a kind of colloidal sediment waste product in the precipitation process using coagulant, an increased amount of SS is produced in large quantities worldwide. SS is reused in landfilling, in forestry, in sea dumping, as soil improver and so on [12,13]. Nevertheless, sometimes it causes a second pollution due to the harmful pollutants that it contains [14]. Given that clean water resources are used to produce the drinking water, the amount of hazardous pollutant in Agadir sewage sludge is relatively low.

* Corresponding author.

1944-3994/1944-3986 © 2017 Desalination Publications. All rights reserved.

In this study, we have analyzed different key factors including pH, initial concentration and contact time to understand the adsorption of cadmium ions onto treated SS of the region of Ait Melloul, Oued Souss, Agadir, Morocco, and adsorption kinetics and isotherm modeling were discussed.

2. Experimental setup

2.1. Preparation of the adsorbent

A desired amount of SS was mixed with a volume of distilled water respecting to ratio of 1:5 ($m_{RM} : V_{DW}$) and pH was adjusted to 3 using H_2SO_4, the mixture was stirred for 12 h. Then, the treated sewage sludge (TSS) was filtered and washed several times with distilled water and ethanol. Finally, the filtered solid (TSS) was heated at 300°C for 4 h.

2.2. Batch adsorption study

Batch adsorption was performed at different initial Cd(II) concentrations to obtain equilibrium isotherms. For isotherm studies, adsorption experiments were carried out by shaking 20 mg of TSS with 250 mL flasks filled with 200 mL of Cd(II) solution at a concentration range 1–5 mg/L at a room temperature for 2 h. After equilibrium, the suspension was filtered and the metal solution then was analyzed using atomic absorption spectrometer (AAS). In order to obtain the adsorption capacity, the amount of ions adsorbed per mass unit of TSS (mg/g) was evaluated using the following expression:

$$Q_e = (C_i - C_e)V/M \quad (1)$$

The removal percentage of Cd(II) was calculated as follows:

$$\% \text{ Removal} = 100\ (C_i - C_i)/C_i \quad (2)$$

where Q_e is the amount of Cd(II) adsorbed at equilibrium (mg/g), C_i is the initial metal ions concentration (mg/L), C_e is the equilibrium metal ions concentration (mg/L), V is the volume of the aqueous phase (L) and M is the amount of the TSS used (g).

The initial pH was adjusted to the required pH value (4–12) by using NaOH and HCl solutions. For adsorption kinetics, the mixture of the test solution 200 mL (5 mg/L) and TSS (20 mg) was stirred in a shaker at 25°C continuously for 2 h. Separate samples for Cd(II) were drawn after 10, 15, 20, 30, 60 and 120 min intervals. The suspension was filtered and then analyzed using AAS.

2.3. Characterizations

2.3.1. Thermogravimetric analyses

Thermogravimetry was performed to determine the dehydration kinetics of the prepared samples. The thermal decomposition of the precursor was followed under air between 25°C and 1,000°C with a rate of 10°C/min.

2.3.2. Scanning electron microscopy

SEM was used to observe the samples morphology. Preliminary images were obtained with a Philips XL30 SEM using a maximum voltage of 20 kV.

2.3.3. FTIR

The Fourier transform infrared spectra of TSS sample were obtained in the mid infrared region (400–4,000 cm^{-1}) using a Shimadzu 4800S. The spectrum was scanned at resolution of 2.0 cm^{-1} and with 20 scanning.

2.3.4. Specific surface area BET and pore size distribution

The Brunauer–Emmett–Teller (BET) surface area (S_{BET}) was determined by the nitrogen adsorption and desorption isotherm, pore size distribution and specific surface area were measured using an Autosorb-1 surface area and pore size analyzer at 77 K.

2.3.5. Atomic absorption spectrometer

A flame atomic absorption spectrometer (AA-7000), equipped with an optical double-beam photometric system is automatically set for flame measurements, and the high-throughput, single-beam photometric system is automatically set for furnace measurements. It possesses a maximum performance for metal detection through optimal adjustment of the light beam and digital filter, and by using optical components that restrict light loss. The wavelength used for monitoring Cd is 324.8 nm.

3. Results and discussion

3.1. Thermogravimetric analyses

Fig. 1 shows the thermogravimetric analyses of both treated and bare SS. Remarkable weight loss of ~58% and ~64% was observed for SS and TSS, respectively. The first

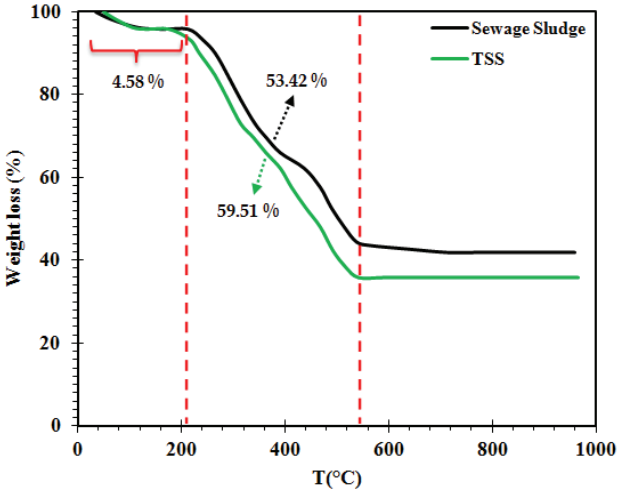

Fig. 1. Thermal decomposition of sewage sludge and treated sewage sludge under air.

weight loss of 4.58% in the range of 50°C–200°C corresponds to the dehydration of the materials meaning the elimination of both surface and lattice water. The second weight loss of 59.51% might be attributed to elimination of different vapors such as NH_3, NO_2 and O_2. The plateau at higher temperatures (i.e., above 600°C) corresponds to some oxide minerals in the samples (SiO_2, MgO and Al_2O_3).

3.2. Scanning electron microscopy

Fig. 2 illustrates the morphology of bare and TSS, it can be clearly seen that the morphology of SS (Fig. 2(a)) consists of rough aggregated micrometric plates with irregular orientations and size. After sulfuric acid activation, the morphology became more regular with rounded aggregated particles.

3.3. FTIR

The Fourier transform infrared spectroscopy (FTIR) spectrum of prepared adsorbent is presented in Fig. 3. The peaks at 3,400, 2,848, 1,442 and 1,627 cm^{-1} are related, respectively, to several organic functional groups such as –OH stretching vibration [15], C–H stretching vibration [16], C=C band, C=O and COO– [17]. These features show the surface carbon structure of the TSS which consists of high content of carboxylic, chain hydrocarbons and aromatic compounds. The peak at 3,400 cm^{-1} might be associated also to the stretching of the N–H bond of organic compounds [12], while the band at ~1,420 cm^{-1} will be attributed to the C–H stretching of CH_2 and CH_3 [15,18]. Additionally, the aromatic rings will promote π-electron bonding which is reported to have a strong affinity with heavy metal cations [19]. The heat treatment at 300°C may have increased the distribution of the functional groups such as –OH and $–CH_2–$ structures. Furthermore, the strong band in the range of 1,030–1,080 cm^{-1} might be attributed to the O–H functional group in mineral components or to the C–O functional group [20,21]. The band around 1,080 cm^{-1} is due to siloxane Si–O–Si and Si–O–C groups [22]. This observation is in agreement with the thermal analyses which shows the existence of mineral oxides in the bare and treated samples. Finally, the weak bands in the region of 760–780 cm^{-1} are associated with the aromatic ring C–H [18].

3.4. BET surface area

Fig. 4 illustrates the nitrogen adsorption–desorption isotherm for the treated sample; reliable analysis of surface area and porosity are obtained. Raw material and TSS have the same adsorption features: the amount of adsorbed quantity has increased after treatment. The adsorption isotherm of the TSS exhibited a type IV isotherm. The hysteresis loop at medium and high pressure can be categorized as H3 in IUPAC classification, this type of loop indicates the existence of disordered mesoporous networks and slit-like pore structure [23,24]. The total pore volume is 0.0361 cm^3/g and the average pore size (aperture) is 3.38 cm^3/g (Table 1) meaning that the TSS has a mesoporous structure which is very suitable for the adsorption of Cd(II) ions in aqueous solution.

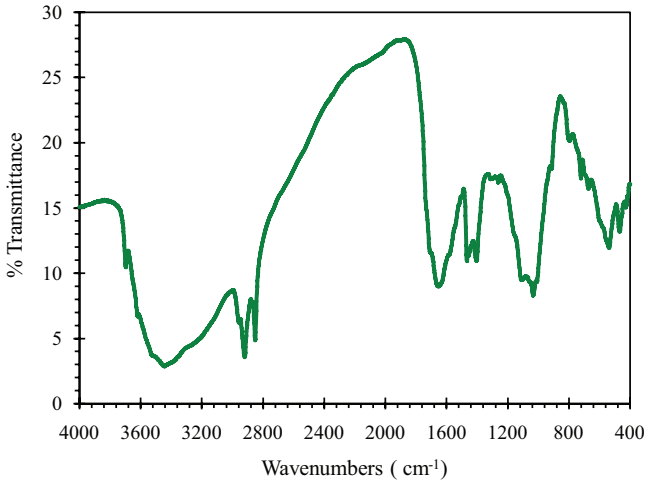

Fig. 3. FTIR of the treated sewage sludge.

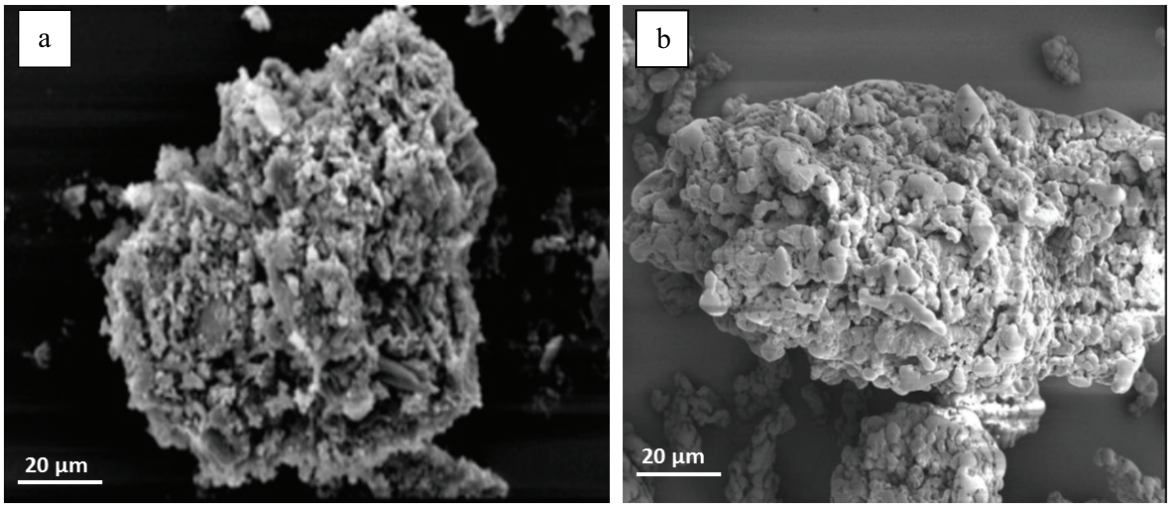

Fig. 2. SEM micrographs of the raw (a) and treated sewage sludge (b).

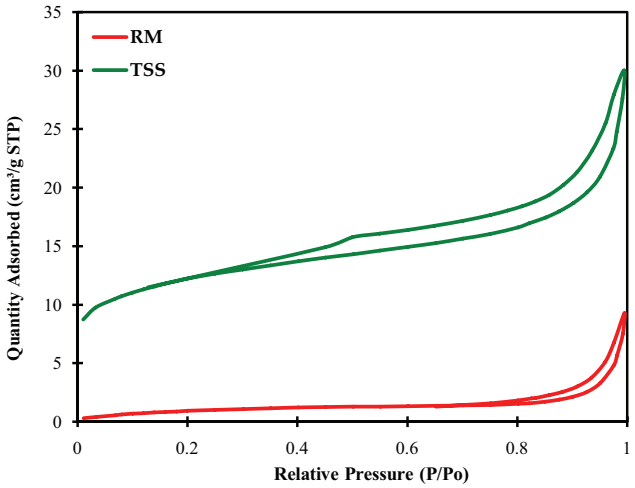

Fig. 4. Nitrogen adsorption–desorption isotherms of the raw material (red) and treated sewage sludge (green).

Table 1
BET surface area and average pore size of the treated sewage sludge

	BET surface area (m^2/g)	Langmuir surface area (m^2/g)	Total pore volume (cm^3/g)	Average pore size (nm)
RM	4	6	0.0075	7.73
TSS	43	58	0.0361	3.38

4. Data analysis

4.1. Equilibrium modeling

Three adsorption isotherm models were used to simulate information about the distribution of adsorbate molecules at the solid–liquid interface. The equilibrium adsorption data were analyzed by Langmuir [25], Freundlich [26] and Temkin [27]; Table 2 highlights the mathematical parameters of the as-cited models.

4.2. Adsorption kinetic models

In order to clarify the adsorption kinetics of cadmium ions onto TSS, the Lagergren pseudo-first-order, pseudo-second-order and intraparticle diffusion kinetic models were applied to fit the present experimental data. The equations of the selected models are listed in Table 3.

5. Adsorption study

5.1. pH effect

It is well known that adsorption and distribution of heavy metal ions on different adsorbents depends on their nature, surface as well as pH of the solution. Fig. 5 shows the pH effect on the removal of Cd(II) using TSS. The removal of cadmium ions increased with increasing pH value; for instance, at low values of pH, the percentage removal is low which is due to the protons competition with metal ion for the binding sites on the TSS surface meaning an important electrostatic repulsion was promoted; at this stage, protons also decrease the negative charges by association of the functional group with protons [33]. As the pH increases, the removal percentage increases as well; this can be associated with the

Table 2
Isotherm models

Isotherm	Equation	Description	References
Langmuir	$1/Q_e = 1/Q_m + 1/(K_L Q_m C_e)$ (3)	C_e = concentration at equilibrium; Q_e = uptake at equilibrium; Q_m = maximum adsorption capacity; K_L = energy of adsorption	[28]
Freundlich	$\ln(Q_e) = \ln K_F + 1/n \ln(C_e)$ (4)	K_F = adsorption capacity; n = intensity of adsorption; $1/n = 0$ irreversible, $1/n > 1$ unfavorable, $0 < 1/n < 1$ favorable	[26]
Temkin	$Q_e = B \ln(A_T C_e)$; $B = RT/b_T$ (5)	R (8.314 J/mol K) universal gas constant; T (K) = temperature; b_T (J/mol), Temkin constant related to heat of sorption; A_T (L/g), Temkin equilibrium binding constant	[29]

Table 3
Kinetic models used to fit the experimental data

Kinetic models	Equation	Description	References
Pseudo-first-order	$\ln(Q_e - Q_t) = \log Q_e - K_1 t/2.303$ (6)	Q_t = uptake at time t, Q_e = uptake at equilibrium, K_1 = rate constant	[30]
Pseudo-second-order	$t/Q_t = 1/(K_2 Q_t^2) + 1/Q_e$	K_2 = rate constant	[31]
Elovich	$Q_t = 1/\beta \ln(\alpha\beta) + 1/\beta \ln t$ (7)	α (mg/g min) = initial sorption rate, and the β parameter (g/mg) is related to the extent of surface coverage	[31]
Intraparticle diffusion	$Q_t = K_{di} t^{0.5} + C$ (8)	K_{di} = rate constant	[32]

decrease of H^+ on the surface, which results in less repulsion with metal ions [34]. According to Fig. 5, the TSS adsorbent presents a maximum removal capacity of Cd(II) in the pH = 6. At higher pH values, soluble hydroxylated complex of cadmium ions enters in a competition with the TSS active sites and therefore the retention decreased [35].

5.2. Initial cadmium concentration effect and contact time

High Cd(II) concentration is always found in the case of industrial wastewater (in the range of mg/L); however, in the case of ground water contamination, the Cd(II) is much lower (in the range of μg/L). Herein, we have studied series of different Cd(II) solutions ranging from 1 to 5 mg/L under the optimized conditions (at pH 6.0, an adsorbent amount of 20 mg and at room temperature for 2 h). The obtained results showed that the removal of Cd(II) is dependent on the initial concentration, the adsorption capacity increases with increase of the initial concentration (Fig. 6) inferring that the cadmium adsorption is processed in specific sites. At higher initial concentration (figure not presented) up to 10 mg/L, we have remarked a sudden drop in the adsorption capacity which is due to the saturated active sites and filled exchange sites and pores [36]. We should note that we have selected 5 mg/L to investigate the effect of contact time. Fig. 6(b) shows that the removal rate of 5 mg/L Cd(II) is higher and rapid in the first 30 min due to the large surface area, mesoporous structure and to the existing of numerous sites and functional radicals on the TSS surface.

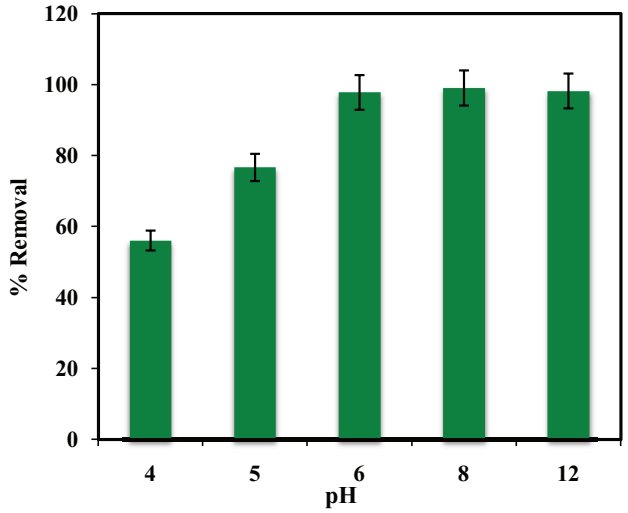

Fig. 5. Effect of pH solution on the removal of Cd(II) by TSS.

5.3. Adsorption kinetics

Linear forms of kinetic models and rate constants along with coefficient of determination (R^2) were used to investigate the interaction between adsorbent–adsorbate.

According to the data modeling presented in Table 4 and Fig. 7, the pseudo-second-order model was found to be the best fit for the experimental study as the values of the correlation coefficients (R^2) were greater than those of the pseudo-first-order and Elovich models. Also, the adsorption capacity predicted by the pseudo-second-order model is closer to that obtained experimentally. This result suggests that the experimental data of the Cd adsorption onto the TSS is governed by the pseudo-second-order model.

The Weber–Morris plot Q_t vs. $t^{1/2}$ (Eq. (6)) was used to understand the diffusion mechanism [34,37]. The plot presented in Fig. 8 gives multilinear aspect, the intraparticular

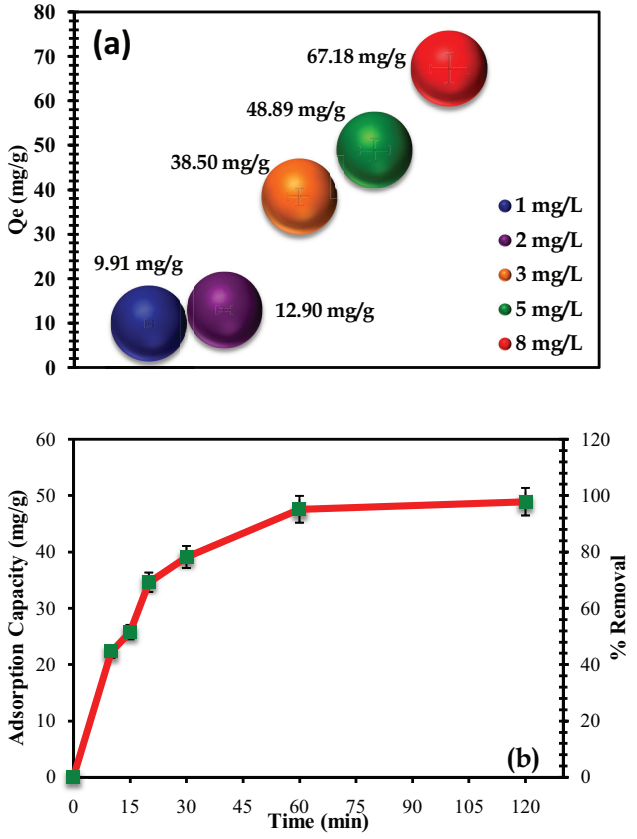

Fig. 6. (a) Initial Cd(II) concentration effect and (b) effect of contact time on the adsorption process.

Table 4
Adsorption kinetic model rate constants for Cd(II) removal

$Q_{e,exp}$ (mg/g)	Pseudo-first-order			Pseudo-second-order			Elovich		
	$Q_{e,cal}$ (mg/g)	K_1 (min^{-1})	R^2	$Q_{e,cal}$ (mg/g)	K_2 (g/mg min)	R^2	α (mg/g min)	β (g/mg)	R^2
48.89	31.38	0.077	0.858	52.63	0.002	0.996	0.071	0.087	0.923
Intraparticle diffusion model									
K_{d1} (mg/g $min^{1/2}$)	C_1 (mg/g)		R^2			K_{d2} (mg/g $min^{1/2}$)		C_2 (mg/g)	R^2
7.2513	0.3027		0.9885			0.4199		44.292	1

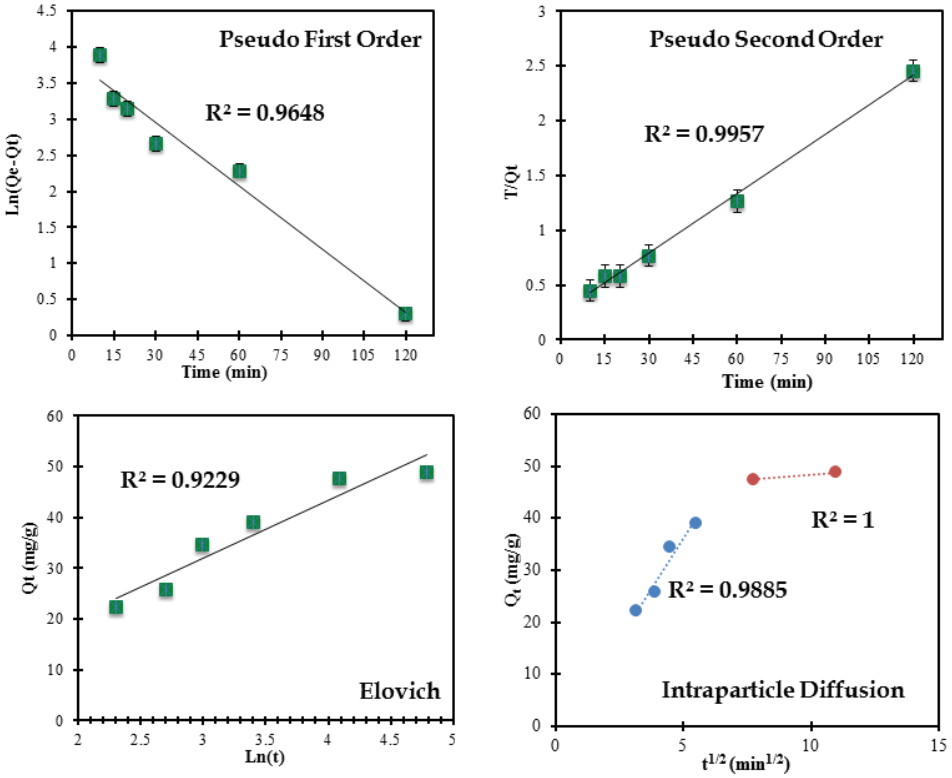

Fig. 7. Kinetic models for Cd(II) adsorption by TSS.

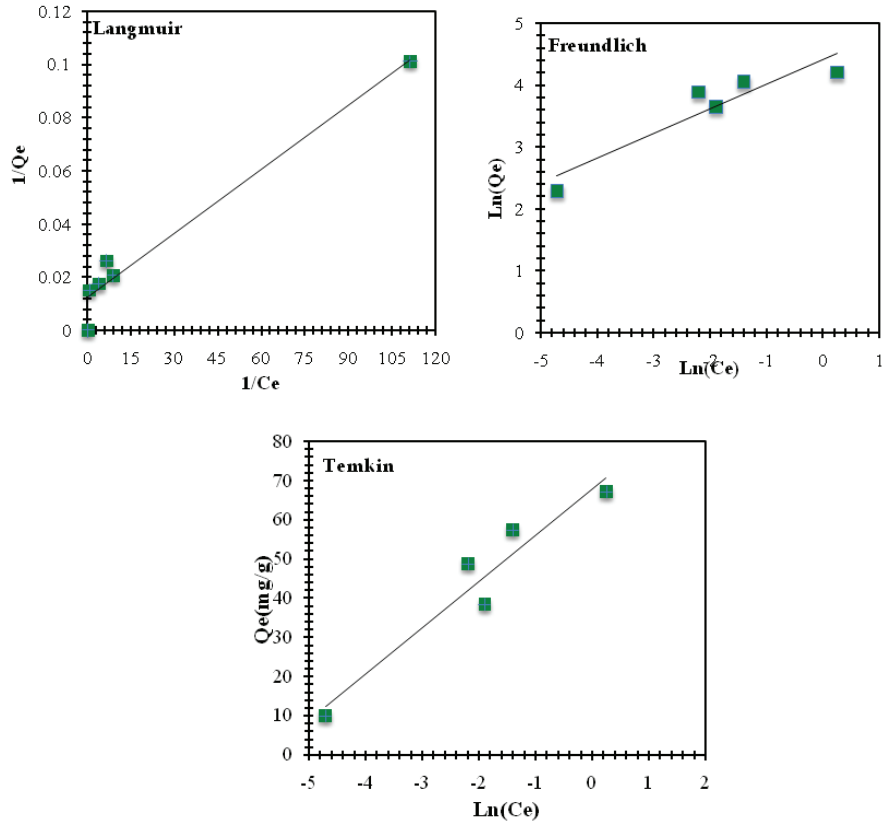

Fig. 8. Langmuir, Freundlich and Temkin isotherm plots for adsorption of Cd(II) on TSS.

diffusion rate (K_{di}) and C were determined from the plot, as one can see there are two steps controlling adsorption:

- The initial stage indicates mass transfer of Cd(II) molecules from the liquid phase to the solid exterior surface (external surface adsorption or boundary layer diffusion).
- The second stage is the intraparticle diffusion: transport of the adsorbate within the pores starts and the equilibrium is established.

The adsorption of cadmium ions onto TSS is a combination of both external surface adsorption and intraparticle diffusion as rate-controlling steps.

5.4. Adsorption isotherm modeling

Isotherm models of Langmuir, Freundlich and Temkin [37] were applied to the adsorption of Cd(II) on TSS at room temperature. The results are shown in Fig. 8 and the isotherm parameters are listed in Table 5.

The Langmuir adsorption capacity, which assumes monolayer adsorption, was equal to 56.2 mg/g. This result is much better than different adsorbent reported in the literature. For instance, Liang et al. [38] have reported a capacity of 7.9 mg/g of the titanium dioxide nanoparticles. Li et al. [39] have utilized carbon nanotubes and indicated an adsorption capacity of 1.1 mg/g. Also, recently Phuengprasop et al. [40] reported an adsorption capacity of 14.7 mg/g of iron oxide coated SS.

Table 5
Comparison of adsorption capacity with other adsorbent

Adsorbent	Adsorption capacity (mg/g)	References
Titanium dioxide nanoparticles	7.9	[38]
Carbon nanotubes (CNTs)	1.1	[39]
Iron oxide coated sewage sludge	14.7	[40]
Commercial activated carbon	2.5	[41]
Waste slurry	15.73	[42]
Banana peel	35.52	[43]
Sugar beet pulp	46.10	[44]
Black gram husk	38.76	[45]
Scolymus hispanicus	54.05	[46]
Activated carbon from coconut coir pith	93.4	[47]
TSS	56.2	This study

Commercial activated carbon which is a common adsorbent in many countries was also studied by Chen et al. [41] giving an adsorption capacity of 2.5 mg/g. The adsorbent used in this study presents a low-cost material with a remarkable adsorption capacity compared with other materials reported earlier. Table 5 highlights a comparison with other materials for the removal of Cd(II).

The essential characteristic of Langmuir isotherm is the dimensionless separation factor which can be expressed as follows [48]:

$$R_L = 1/(1 + K_L C_0) \quad (9)$$

where C_0 is the initial concentration (mg/L) and b is the Langmuir constant (L/mg). The value of R_L was found to 0.0049 indicating that the adsorption of Cd(II) on TSS is favorable. In contrast to the Langmuir isotherm, Freundlich isotherm is derived by assuming heterogeneous surface of studied adsorbent TSS [49]. The value of Freundlich constant N is found to be 3.997 implying that cadmium mass was adsorbed instantaneously. This confirms a favorable adsorption of cadmium on the TSS.

Temkin isotherm constant A_T is related to the bending of adsorbate–adsorbent at equilibrium corresponding to maximum binding energy and b_T is associated with heat of adsorption. The b_T value for Cd(II) adsorption on TSS is 0.206 kJ/mol meaning that the adsorption process is physical in nature. Based on these experimental data, the adsorption of Cd(II) on TSS is physisorption process. The obtained values of R^2, presented in Table 6, signify the applicability of Langmuir followed by Temkin isotherm to experimental data. The fitting of the two isotherms reflects the homogeneous surface of TSS (Fig. 8).

5.5. Adsorption mechanism

Table 7 presents the elemental analyses of the TSS after and before adsorption of Cd ions. Elemental analyses clearly confirm the presence of cadmium ions on the surface of the support. Fig. 9 reports the FTIR of the TSS before and after adsorption, a significant increase of the intensities band was observed in the region of the –OH stretching vibration at 3,400 cm^{-1} when compared with the pristine TSS, this can be due to the adsorbed water after adsorption. Additionally, all the others bands in the region 200–2,600 cm^{-1} were found to be decreased in intensity; this might be due to the electrostatic interactions between the functional groups COO–, –NH and –CO and cadmium ions [50,51]. This phenomenon was also reported by Gutiérrez-Segura et al. [52] when they studied the removal of cadmium by Na- and Fe-modified zeolitic tuffs and carbonaceous material from pyrolyzed SS. These results can serve as clear evidence of the removal of Cd ions by the TSS.

Table 6
Langmuir, Freundlich and Temkin constants for adsorption of Cd(II) on TSS

Langmuir				Freundlich			Temkin			
Q_{max} (mg/g)	K_L (L mg^{-1})	R_L	R^2	K_F (mg/g)	N	R^2	A_T (L/mg)	B	b_T (J/mol)	R^2
56.2	25.43	0.0049	0.9800	54.32	3.997	0.5542	317.29	11.791	206.598	0.9201

Table 7
Elemental analyses of the TSS before and after adsorption of Cd (ions)

Elements	TSS before adsorption	TSS after adsorption
C (%)	39.76	36.81
O (%)	43.36	45.26
H (%)	5.93	6.09
N (%)	4.03	4.32
S (%)	2.01	1.43
Ash (%)	24.70	21.10
Other (Si, Fe and Al) (%)	4.91	4.68
Cd (%)	–	1.22

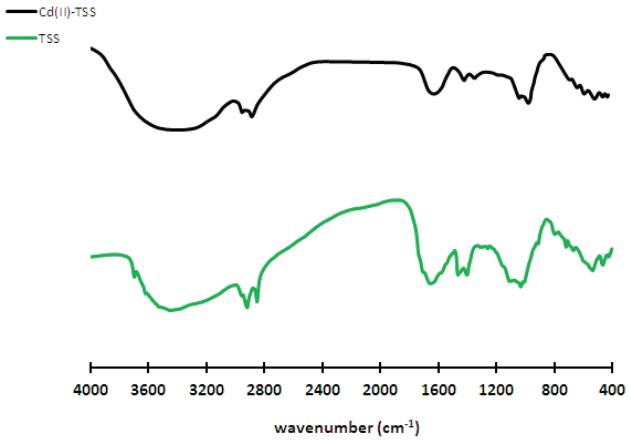

Fig. 9. FTIR of TSS after and before Cd(II) removal.

6. Conclusion

The adsorption of cadmium ions onto TSS was described by the pseudo-second-order model and Langmuir isotherm. Batch adsorption experiments can be affected by various key parameters such as contact time, solution pH and initial metal ion concentration. The TSS presented a higher Cd(II) uptake than different low-cost adsorbent described in the literature even at 5 ppm of cadmium ions concentration. The TSS adsorbent yielded an adsorption capacity of the 56.2 mg/g due to its high BET surface area, mesoporous structure and availability of different functional groups acting as chelating agent to adsorb heavy metal ions through different approaches. Thus, the TSS can be used as an efficient low-cost adsorbent for the removal of cadmium ions even in small quantities (in the range of 5 ppm).

Acknowledgment

The authors would like to acknowledge the support of the Ibn Zohr University.

Conflict of interest

On behalf of all authors, the corresponding author states that there is no conflict of interest.

References

[1] J. Wang, C. Chen, Biosorbents for heavy metals removal and their future, Biotechnol. Adv., 27 (2009) 195–226.
[2] M. Kılıç, Ç. Kırbıyık, Ö. Çepelioğullar, A.E. Pütün, Adsorption of heavy metal ions from aqueous solutions by bio-char, a by-product of pyrolysis, Appl. Surf. Sci., 283 (2013) 856–862.
[3] A.R. Agg, T.F. Zabel, EC directive on the control of dangerous substances (76/464/EEC): its impact on the UK water industry, Water Environ. J., 3 (1989) 436–442.
[4] ELINCS new substances list, Anal. Proc., 28 (1991) 348.
[5] D. Sud, G. Mahajan, M.P. Kaur, Agricultural waste material as potential adsorbent for sequestering heavy metal ions from aqueous solutions – a review, Bioresour. Technol., 99 (2008) 6017–6027.
[6] H.S. Ernst, K.S. Minamyer, K.R. Fox, EPA Drinking Water Security Research Program, R.M. Clark, S. Hakim, A. Ostfeld, Eds., Handbook of Water and Wastewater Systems Protection, Springer New York, New York, NY, 2011, pp. 47–64.
[7] S.S. Pillai, B. Deepa, E. Abraham, N. Girija, P. Geetha, L. Jacob, M. Koshy, Biosorption of Cd(II) from aqueous solution using xanthated nano banana cellulose: equilibrium and kinetic studies, Ecotoxicol. Environ. Saf., 98 (2013) 352–360.
[8] C. Namasivayam, E.C. Division, Removal of Cd(II) from wastewater by adsorption on "waste" Fe(III)/Cr(III) hydroxide, Water Res., 29 (1995) 1737–1744.
[9] N. Barka, M. Abdennouri, M. El Makhfouk, S. Qourzal, Biosorption characteristics of cadmium and lead onto eco-friendly dried cactus (*Opuntia ficus-indica*) cladodes, J. Environ. Chem. Eng., 1 (2013) 144–149.
[10] J.-L. Hu, X.-W. He, C.-R. Wang, J.-W. Li, C.-H. Zhang, Cadmium adsorption characteristic of alkali modified sewage sludge, Bioresour. Technol., 121 (2012) 25–30.
[11] W. Zou, H. Bai, S. Gao, Competitive adsorption of neutral red and Cu^{2+} onto pyrolytic char: isotherm and kinetic study, J. Chem. Eng. Data, 57 (2012) 2792–2801.
[12] S.E.A.S. El-Deen, F.-S. Zhang, Immobilisation of TiO_2-nanoparticles on sewage sludge and their adsorption for cadmium removal from aqueous solutions, J. Exp. Nanosci., 11 (2016) 239–258.
[13] S. Ishikawa, N. Ueda, Y. Okumura, Y. Iida, K. Baba, Recovery of coagulant from water supply plant sludge and its effect on clarification, J. Mater. Cycles Waste Manage., 9 (2007) 167–172.
[14] X. Chen, S. Jeyaseelan, N. Graham, Physical and chemical properties study of the activated carbon made from sewage sludge, Waste Manage., 22 (2002) 755–760.
[15] Z. Droussi, V. D'orazio, M.R. Provenzano, M. Hafidi, A. Ouatmane, Study of the biodegradation and transformation of olive-mill residues during composting using FTIR spectroscopy and differential scanning calorimetry, J. Hazard. Mater., 164 (2009) 1281–1285.
[16] J. Pan, G. Li, Z. Chen, X. Chen, W. Zhu, K. Xu, Alternative block polyurethanes based on poly(3-hydroxybutyrate-co-4-hydroxybutyrate) and poly(ethylene glycol), Biomaterials, 30 (2009) 2975–2984.
[17] Q. Chen, D. Yin, S. Zhu, X. Hu, Adsorption of cadmium(II) on humic acid coated titanium dioxide, J. Colloid Interface Sci., 367 (2012) 241–248.
[18] X.J. Beiping Zhang, S. Xiong, B. Xiao, D. Yu, Mechanism of wet sewage sludge pyrolysis in a tubular furnace, Int. J. Hydrogen Energy, 36 (2011) 355–363.
[19] O.R. Harvey, B.E. Herbert, R.D. Rhue, L.-J. Kuo, Metal interactions at the biochar-water interface: energetics and structure-sorption relationships elucidated by flow adsorption microcalorimetry, Environ. Sci. Technol., 45 (2011) 5550–5556.
[20] H.J. Percival, J.F. Duncan, P.K. Foster, Interpretation of the kaolinite-mullite reaction sequence from infrared absorption spectra, J. Am. Ceram. Soc., 57 (1974) 57–61.
[21] G. Liu, H. Song, J. Wu, Thermogravimetric study and kinetic analysis of dried industrial sludge pyrolysis, Waste Manage., 41 (2015) 128–133.

[22] L. Gu, N. Zhu, H. Guo, S. Huang, Z. Lou, H. Yuan, Adsorption and Fenton-like degradation of naphthalene dye intermediate on sewage sludge derived porous carbon, J. Hazard. Mater., 246–247 (2013) 145–153.
[23] R. Haul, S.J. Gregg, K.S.W. Sing, Adsorption, Surface Area and Porosity. 2. Auflage, Academic Press, London 1982. 303 Seiten, Berichte Der Bunsengesellschaft Für Phys. Chemie., 86 (1982) 957.
[24] T. Sivakumar Natarajan, H.C. Bajaj, R.J. Tayade, Synthesis of homogeneous sphere-like Bi_2WO_6 nanostructure by silica protected calcination with high visible-light-driven photocatalytic activity under direct sunlight, CrystEngComm, 17 (2015) 1037–1049.
[25] I. Langmuir, The adsorption of gases on plane surfaces of glass, mica and platinum, J. Am. Chem. Soc., 40 (1918) 1361–1403.
[26] H.M.F. Freundlich, Over the adsorption in solution, J. Phys. Chem., 57 (1906) 385–471.
[27] B.H. Hameed, A.A. Rahman, Removal of phenol from aqueous solutions by adsorption onto activated carbon prepared from biomass material, J. Hazard. Mater., 160 (2008) 576–581.
[28] Langmuir Irving, The adsorption of gases on plane surfaces of glass, mica and platinum, J. Am. Chem. Soc., 40 (1918) 1361.
[29] B.H. Hameed, D.K. Mahmoud, A.L. Ahmad, Sorption equilibrium and kinetics of basic dye from aqueous solution using banana stalk waste, J. Hazard. Mater., 158 (2008) 499–506.
[30] L.S, Zur theorie der sogenannten adsorption gelöster stoffe [On the theory of so-called adsorption of dissolved substances], K. Sven. Vetensk.akad., Handl., 24 (1898) 1.
[31] Y. Khambhaty, K. Mody, S. Basha, B. Jha, Kinetics, equilibrium and thermodynamic studies on biosorption of hexavalent chromium by dead fungal biomass of marine *Aspergillus niger*, Chem. Eng. J., 145 (2009) 489–495.
[32] W.J. Weber, J.C. Morris, Kinetics of adsorption carbon from solutions, J. Sanit. Eng. Div. Proc. Am. Soc. Civ. Eng., 89 (1963) 31–60.
[33] L. Khalfa, M. Bagane, Cadmium removal from aqueous solution by a Tunisian smectitic natural and activated clay: thermodynamic study, J. Encapsulation Adsorpt. Sci., 1 (2011) 65–71.
[34] R.R. Sheha, A.A. El-Zahhar, Synthesis of some ferromagnetic composite resins and their metal removal characteristics in aqueous solutions, J. Hazard. Mater., 150 (2008) 795–803.
[35] R. Vimala, N. Das, Biosorption of cadmium (II) and lead (II) from aqueous solutions using mushrooms: a comparative study, J. Hazard. Mater., 168 (2009) 376–382.
[36] N. Li, L. Zhang, Y. Chen, Y. Tian, H. Wang, Adsorption behavior of Cu(II) onto titanate nanofibers prepared by alkali treatment, J. Hazard. Mater., 189 (2011) 265–272.
[37] M.H. Kalavathy, T. Karthikeyan, S. Rajgopal, L.R. Miranda, Kinetic and isotherm studies of Cu(II) adsorption onto H_3PO_4-activated rubber wood sawdust, J. Colloid Interface Sci., 292 (2005) 354–362.
[38] P. Liang, T. Shi, J. Li, Nanometer-size titanium dioxide separation/preconcentration and FAAS determination of trace Zn and Cd in water sample, Int. J. Environ. Anal. Chem., 84 (2004) 315–321.
[39] Y.-H. Li, S. Wang, Z. Luan, J. Ding, C. Xu, D. Wu, Adsorption of cadmium(II) from aqueous solution by surface oxidized carbon nanotubes, Carbon, 41 (2003) 1057–1062.
[40] T. Phuengprasop, J. Sittiwong, F. Unob, Removal of heavy metal ions by iron oxide coated sewage sludge, J. Hazard. Mater., 186 (2011) 502–507.
[41] T. Chen, Y. Zhang, H. Wang, W. Lu, Z. Zhou, Y. Zhang, L. Ren, Influence of pyrolysis temperature on characteristics and heavy metal adsorptive performance of biochar derived from municipal sewage sludge, Bioresour. Technol., 164 (2014) 47–54.
[42] T.J. Bandosz, Activated carbon surfaces in environmental remediation, Interface Sci. Technol., 7 (2006) 571.
[43] J.R. Memon, S.Q. Memon, M.I. Bhanger, G.Z. Memon, A. El-Turki, G.C. Allen, Characterization of banana peel by scanning electron microscopy and FT-IR spectroscopy and its use for cadmium removal, Colloids Surf., B, 66 (2008) 260–265.
[44] E. Pehlivan, B.H. Yanık, G. Ahmetli, M. Pehlivan, Equilibrium isotherm studies for the uptake of cadmium and lead ions onto sugar beet pulp, Bioresour. Technol., 99 (2008) 3520–3527.
[45] A. Saeed, M. Iqbal, Bioremoval of cadmium from aqueous solution by black gram husk (*Cicer arientinum*), Water Res., 37 (2003) 3472–3480.
[46] N. Barka, M. Abdennouri, A. Boussaoud, M.E.L. Makhfouk, Biosorption characteristics of cadmium(II) onto *Scolymus hispanicus* L. as low-cost natural biosorbent, Desalination, 258 (2010) 66–71.
[47] K. Kadirvelu, C. Namasivayam, Activated carbon from coconut coirpith as metal adsorbent: adsorption of Cd(II) from aqueous solution, Adv. Environ. Res., 7 (2003) 471–478.
[48] A. Kamari, S.N.M. Yusoff, F. Abdullah, W.P. Putra, Biosorptive removal of Cu(II), Ni(II) and Pb(II) ions from aqueous solutions using coconut dregs residue: adsorption and characterisation studies, J. Environ. Chem. Eng., 2 (2014) 1912–1919.
[49] D. Ova, B. Ovez, 2,4-Dichlorophenoxyacetic acid removal from aqueous solutions via adsorption in the presence of biological contamination, J. Environ. Chem. Eng., 1 (2013) 813–821.
[50] S.E. Manahan Chemical Analysis of Water and Wastewater, in: Environmental Chemistry, 7th ed., CRC Press, 1999.
[51] S.E. Manahan Analysis of Wastes and Solids, in: Environmental Chemistry, 7th ed., CRC Press, 1999.
[52] E. Gutiérrez-Segura, M. Solache-Ríos, A. Colín-Cruz, C. Fall, Adsorption of cadmium by Na and Fe modified zeolitic tuffs and carbonaceous material from pyrolyzed sewage sludge, J. Environ. Manage., 97 (2012) 6–13.